# Ultracentrifugal subclasses of low and intermediate density lipoproteins

**Jan J. Opplt**[1] **and Evan S. Holzberg**

Case Western Reserve University, Cleveland State University, Cleveland, OH 44136

**Abstract** Low density lipoprotein (LDL) and intermediate density lipoprotein (IDL) classes have been shown to be composed of discrete metabolic entities or subclasses. Present ultracentrifugal methods are unable to precisely determine these subclasses. A new analytical micro-ultracentrifugal method was developed that facilitates the determination of IDL and LDL subclasses and their $F_{1.21}$ flotation coefficient from ultracentrifugal scans. The method is based on the modification of a published equation (Fujita, H. 1956. *J. Chem. Phys.* **24:** 1084–1090) adapted to calculate concentration gradient boundary curves for IDL and LDL that are approximately Gaussian in form. Using an extension of this modified equation, theoretical distributions of the gradient curves were calculated. By applying the theoretical distributions, IDL and LDL subclasses were resolved from absorbance scans as Gaussian concentration gradient boundary curves. Both theoretically calculated and experimentally determined boundary curves for IDL and LDL lipoproteins were plotted and found to be in excellent agreement. Three subclasses of LDL and four subclasses of IDL were determined. The mean flotation rates of the LDL subclasses were: $LDL_1$ = 37.2 ± 0.6, $LDL_2$ = 31.1 ± 0.9, and $LDL_3$ = 26.7 ± 0.7. The mean flotation rates of the IDL subclasses were: $IDL_1$ = 61.6 ± 0.9, $IDL_2$ = 53.9 ± 1.0, $IDL_3$ = 50.1 ± 0.6, and $IDL_4$ = 45.6 ± 1.1.—**Opplt, J. J., and E. S. Holzberg.** Ultracentrifugal subclasses of low and intermediate density lipoproteins. *J. Lipid Res.* 1994. **35:** 510–523.

**Supplementary key words** flotation • concentration gradient curve • boundary curves

Human LDL, d 1.019–1.063 g/ml, $F_{1.21}$ 25–40[2] are now recognized to be a heterogeneous family of macromolecules varying in physicochemical properties (1–10). The existence of distinctive subclasses of LDL has been reported (6, 10–14). Similarly, the heterogeneity of IDL, d 1.006–1.019 g/ml, $F_{1.21}$ 40–70, and the existence of their subclasses have been indicated (15).

Various ultracentrifugal methods have been presented for isolation of subfractions of LDL (11–13) and IDL (15). Yet, due to the inherent density similarity of the subclasses, these methods are not able to accurately separate and quantify them. Moreover, while both IDL and LDL have been determined to be atherogenic, the pathogenetic significance of their subclasses is still to be better understood.

In this report we describe an ultracentrifugal method for the determination of LDL and IDL subclasses from ultracentrifugal flotation patterns. Analytical ultracentrifugal flotation patterns represent distribution curves of lipoproteins separated on the basis of buoyant density differences, and thus provide a sensitive criterion for observing the heterogeneity and polydispersity of plasma lipoproteins. Characteristic of flotation patterns is the boundary, a region in which concentration varies with distance from the axis of rotation in an analytical cell.

Until now, lipoprotein heterogeneity could only be estimated from boundaries, due to the limitation of available techniques for analysis of boundaries. These include the methods of Swinkels, Hak-Lemmers, and Demacker (13), Ewing, Freeman, and Lindgren (16), Oncley (17), and Anderson et al. (18). They are all time-consuming and/or imprecise due to the lack of applicability of physical distribution characteristics of lipoproteins during ultracentrifugation.

The method we are introducing for resolution of LDL and IDL heterogeneity uses a published equation (19, 20) originally developed by Fujita (19) for determining boundary distributions of sedimenting proteins. By modifying this equation, we obtained an equation that calculates the theoretical diffusive broadening of lipoprotein concentration gradient curves during ultracentrifugation. We used the modified equation to develop a method that resolves LDL and IDL boundary curves into their subclass components. In this report, we have applied and evaluated the developed method for the determination of human LDL and IDL subclasses.

---

Abbreviations: VLDL, very low density lipoprotein; IDL, intermediate density lipoprotein; LDL, low density lipoprotein; HDL, high density lipoprotein.

[1]To whom correspondence should be addressed at: Institute of Pathology, Case Western Reserve University, 2085 Adelbert Road, Cleveland, OH 44106.

[2]$F_{1.21}$, equivalent to $-S_{1.21}$, represents the rate of lipoprotein flotation in a salt medium of density 1.21 g/ml.

In the development of the method, two assumptions were applied. First, that the boundary region of IDL and LDL represents the summation of boundary curves of IDL and LDL subclasses, and secondly, that the shape of the IDL and LDL boundary is due primarily to heterogeneity of the classes and to diffusive broadening of the boundary curves of subclasses.

## MATERIALS AND METHODS

### Clinical data

The subjects selected for this study were part of two larger clinical metabolic studies: A) 17 patients from a study on guanadrel (n = 101), and B) 13 patients enrolled from a study on probucol (n = 47). Six individuals with observed normal lipid and lipoprotein values served as a preliminary reference group.

Study A. The 17 subjects from our clinical pilot study "Guanadrel effects on lipoprotein metabolism in hypertensive patients," had moderate hypertension, mild dyslipoproteinemia, and hyperlipidemia and were exempt of myocardial infarctions or clinically manifest coronary artery disease (CAD) and were not taking any medications known to alter the metabolism of lipids and/or lipoproteins.

Guanadrel therapy was initiated (5 mg per day), and maintained over a 3-month period.[3] During this time, the subjects were kept on a constant diet. Every subject was examined before and after 3 months of therapy with guanadrel.

Study B. The 13 subjects from our clinical pilot study "Effects of probucol on metabolism of lipoproteins in patients with proven coronary artery disease" were characterized by angiographically proven atherosclerotic obstructions of one or more coronary arteries, and related severe, or very severe dyslipoproteinemia and hyperlipidemia. However, none of these patients had any history of a clinically significant myocardial infarction.

All patients required dietary instructions for their dyslipoproteinemia and hyperlipemia during the 6 months prior to this study. This diet was also observed during the 3 months of long experimental therapy with probucol standardly administered (2 × 500 mg per day) (21).

### Sample preparation

Blood samples were collected in tubes, without an anticoagulant, from subjects before the start of either guanadrel or probucol and 12 weeks after drug therapy. The samples were obtained after the subjects had fasted for a minimum of 12 h. The blood was centrifuged, and serum was separated.

### Absorbance scans of IDL and LDL

Lipoproteins were first isolated from serum according to the method of Lewis, Green, and Page (22) at a final density of 1.21 g/ml using KBr and NaCl salts for density adjustment.

Analytical ultracentrifugation of lipoproteins was performed as previously described by Opplt and Bahler (23), at density 1.21 g/ml in a Beckman Model L5-75 ultracentrifuge equipped with UV-scanner assembly and electronic Angular Velocity Integrator ($\omega^2t$). A 12-mm pathlength double sector centerpiece made of aluminum-filled epon and quartz windows were used in the cell.

Cell scans of IDL and LDL were initiated at an angular velocity of $\omega^2t = 2098 \cdot 10^7$ rad²/sec and a rotor speed of 52,640 rpm, and recorded as absorbance versus $\omega^2t$ (the integrated angular velocity of the rotor as read from the instrument's $\omega^2t$ integrator, in radians²/sec). Utilizing previously determined radial positions of IDL and LDL class limits (24), IDL and LDL classes were isolated on recorded $\omega^2t = 2098 \cdot 10^7$ rad²/sec absorbance scans.

### Theoretical concentration distribution of IDL and LDL boundaries

Boundary patterns of sedimenting proteins were predicted by Faxen (25), Fujita (19), and Williams et al. (20) using theoretical equations to form Gaussian concentration gradient curves. By using modifications of Fujita's equation (Eq. 1 in the Appendix), Eq. 2 in the appendix is obtained and used for deriving theoretical IDL and LDL concentration gradient boundary curves. Theoretical boundary curves were derived in their concentration gradient form via Eq. 2 (see Appendix for calculations) for IDL and LDL species with $F_{1.21}$ flotation coefficients of 70, 60, 50, 40, 30, and 20, respectively.

The theoretical concentration distribution of IDL and LDL boundaries was calculated using an extension of Eq. 2 (see Eq. 4 in Appendix). Plots of the percentage distribution for IDL and LDL boundaries at specified distances from the boundary apex position ($r_\star$) were constructed by plotting the calculated concentration percentage distribution for specific boundaries versus the $F_{1.21}$ flotation coefficient of the boundary; $r_\star$ represents the actual radial distance in an analytical cell from the axis of rotation to the apex of the boundary.

### Graphic representation of experimental IDL and LDL subclasses

IDL and LDL subclasses were resolved from recorded $\omega^2t = 2098 \cdot 10^7$ rad²/sec cell scans of absorbance versus $\omega^2t$ (radial distance in the cell) by determining their cor-

[3]The guanadrel sulfate, HYLOREL®-Pennwalt is a postganglionic sympathetic inhibitor (1,4-dioxaspiro-4,5-decan-2-ylmethyl guanadine sulfate). Guanadrel sulfate lowers arterial blood pressure by inhibiting release of the adrenergic transmitter, norepinephrine, from sympathetic nerve terminals and by depleting norepinephrine in neuronal storage sites.

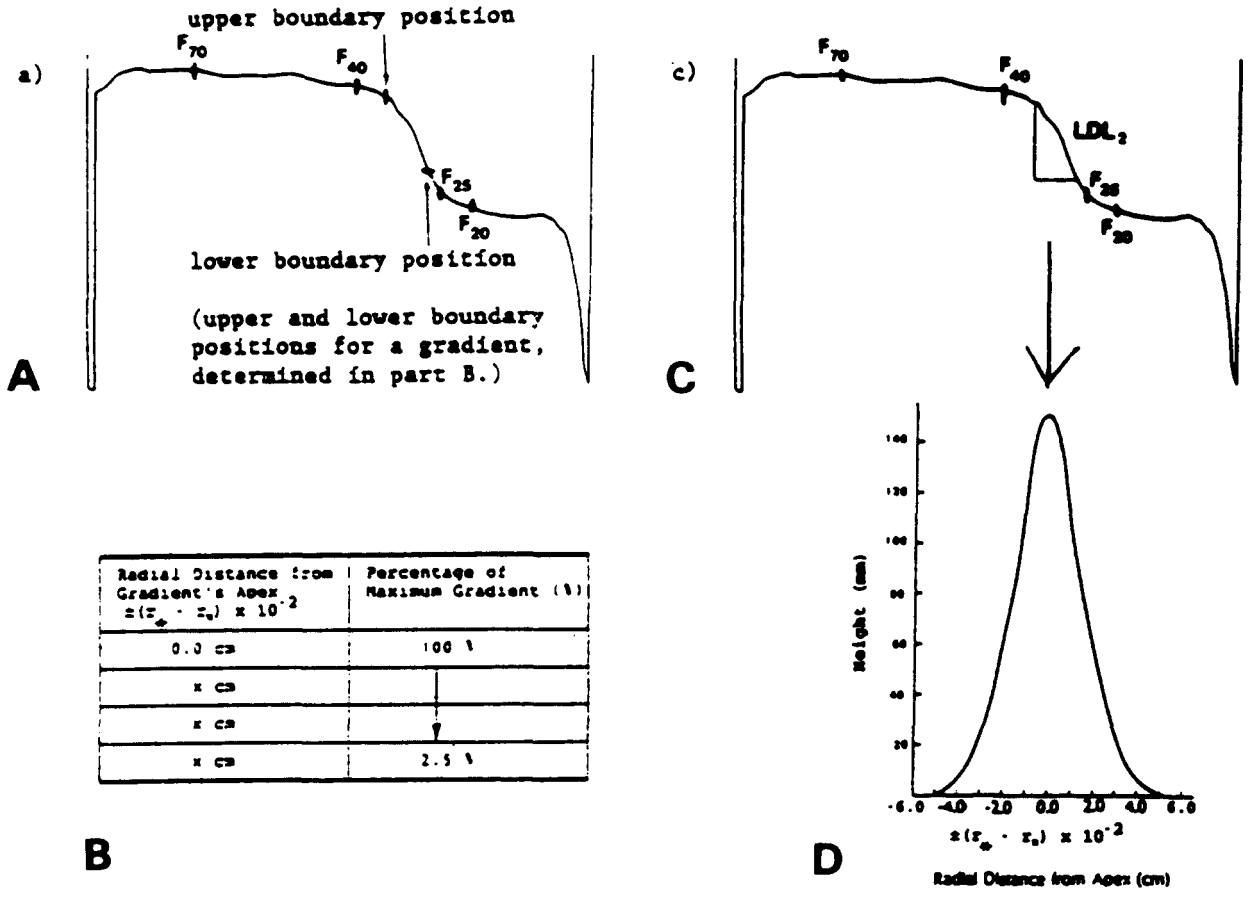


**Fig. 1.** Scheme for deriving boundary curves of IDL and LDL subclasses. A: Determined apex, upper and lower boundary positions. B: Calculated *percentage distribution of concentration gradient from apex position.* C: Determined boundary height. D: Derived Gaussian concentration gradient form of LDL subclass boundary curve.

responding concentration gradient boundary curves as shown in **Fig. 1,** (see Appendix for resolution procedure).

Comparisons of the resolved boundary curves (x-axis in radial distance) versus the $\omega^2t = 2098 \cdot 10^7$ absorbance scan (x-axis in $\omega^2t$ values) were derived by using the relationship of $\omega^2t$ values and radial distance (24). The height of the subclass boundary curves (in mm) versus $\omega^2t$ values was transferred into a computer, in order to facilitate the calculation of the plot of the boundary curves versus $\omega^2t$ readings.

A smooth curve was drawn to represent the derived IDL and LDL subclass boundary curves. The curve was then transposed onto clear plastic. This pattern was then placed over the plot of the first derivative of the experimental scan as a means to measure differences between the two curves.

The derived concentration gradient boundary curves were converted into concentration curves and then graphed versus the $2098 \cdot 10^7$ $\omega^2t$ experimental scan, as well as versus the concentration gradient curves.

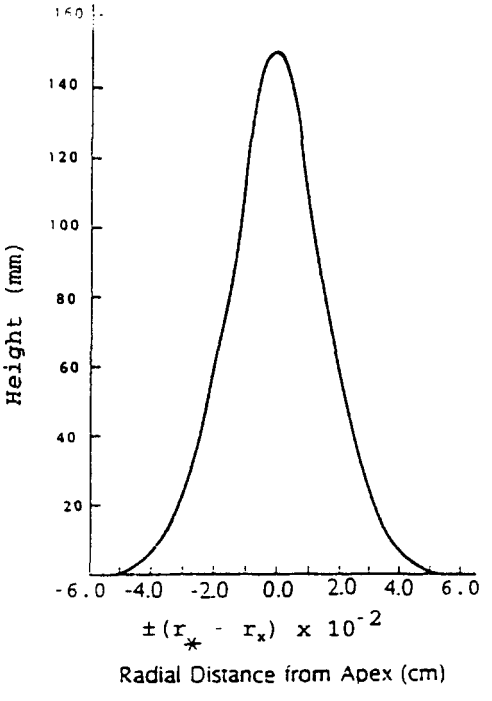


**Fig. 2.** Calculated theoretical boundary concentration gradient curve for $F_{1.21}$ 40 lipoprotein.

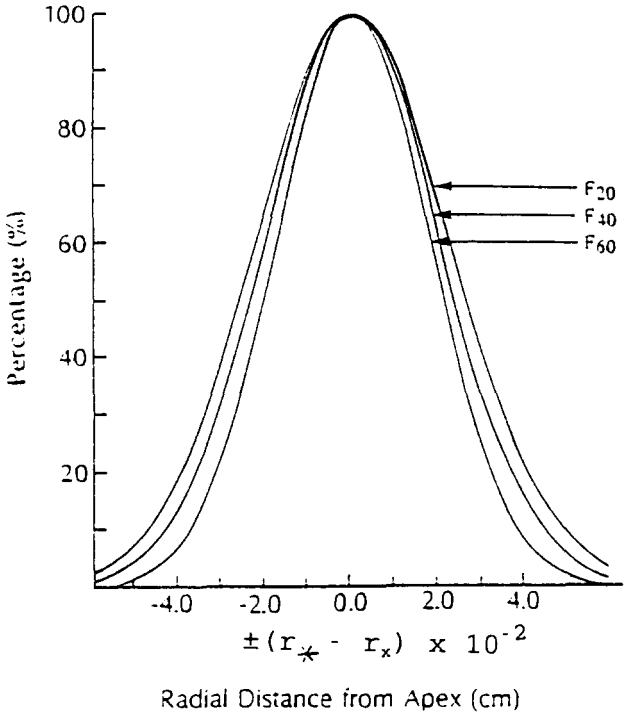


**Fig. 3.** Percentage of the maximum value of gradient curves at specified distances from their apex.

### Theoretical IDL and LDL concentration gradient boundary curves

The derived concentration gradient boundary curves were observed to have a Gaussian distribution about the apex as shown in **Fig. 2** for one boundary curve, with $r_\star - r_x$ representing the radial distance from the apex; $r_x$ represents radial position in the analytical cell, the actual distance from the axis of rotation to the position in the cell.

### Theoretical concentration distribution of IDL and LDL boundaries

The theoretical distribution of three theoretical boundaries (within the $F_{1.21}$ flotation coefficient range defined for LDL and IDL) were calculated from Eq. 4 (Appendix) and graphed as shown in **Fig. 3.**

We observed that the distribution for the $F_{20}$ boundary was broader than that for the $F_{60}$ boundary. The observed differences were attributable to diffusion. The boundaries from the slower flotating lipoprotein species (with smaller flotation coefficients, e.g., $F_{20}$), show greater broadening, due to diffusion.

Plotting the calculated concentration distribution of IDL and LDL boundaries for specific distances $\pm (r_\star - r_x)$ from the boundary apex versus $F_{1.21}$ flotation coefficient of the boundary yielded a sequence of linear decreasing relationships. The concentration gradient percentage at radial distances from the boundary apex increased with decreasing flotation coefficient, demonstrating the concentration broadening effects caused by diffusion.

### Boundary curves of IDL and LDL subclasses

Linear 2098 : $10^7$ $\omega^2$t scans of UV absorbance versus $\omega^2$t positions were converted into first derivative scans, and maxima were determined. The observed maximum were assumed to represent the apex ($r_\star$) of IDL and LDL subclass concentration gradient boundary curves.

$F_{1.21}$ flotation coefficients were calculated for each $r_\star$ position, and then the corresponding concentration gradient boundary curves were derived and graphed (as described in Methods).

Plots of the combined Gaussian concentration boundary curves versus the first derivative of experimental absorbance scans for the IDL to LDL flotation coefficient range were seen to be approximately comparable (**Fig. 4**). This was taken as evidence that recorded absorbance

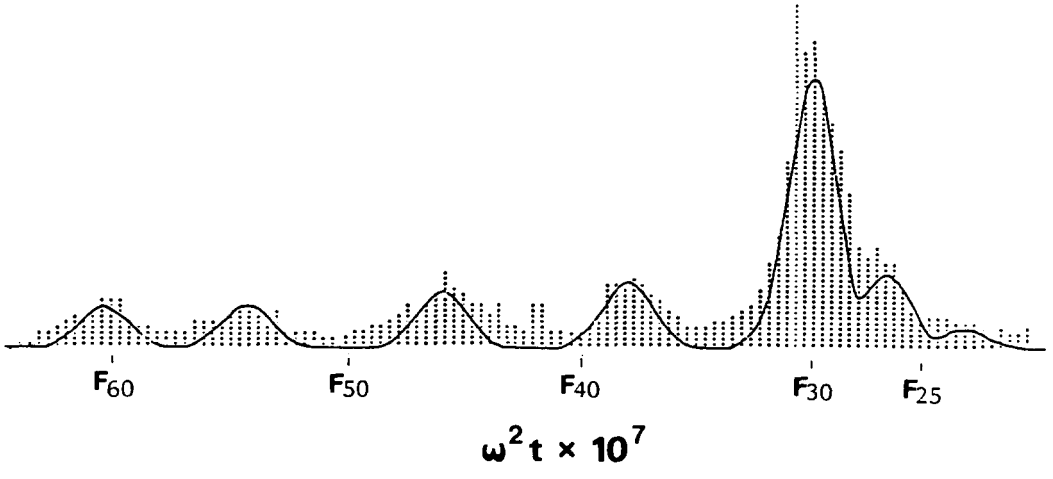


**Fig. 4.** Comparison of Gaussian concentration boundary curves with the first derivative of experimental absorbance scan.

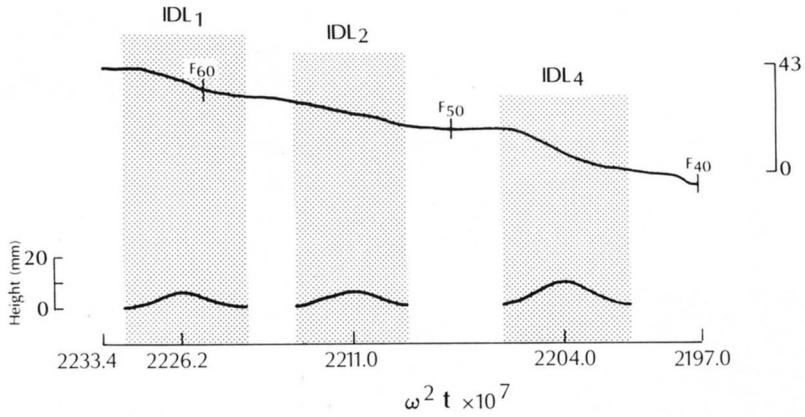


**Fig. 5.** Experimental absorbance curve versus calculated Gaussian concentration gradient curves for IDL subclasses.

scans of IDL and LDL classes represent the summation of boundary curves of IDL and LDL subclasses.

It is significant that the base lengths of the calculated concentration gradient boundary curves were approximately equal to the distance between inflection points on the linear absorbance scan. This indicates that the apex of gradient curves is approximately one-half the distance between inflection points on the experimental scan. This becomes the basis for using inflection points to determine boundary apexes. Graphic representations of the derived Gaussian concentration gradient boundary (below the experimental scan) are shown on **Fig. 5** for the IDL class, and on **Fig. 6** for the LDL class.

In another series of experiments, the concentration gradient curves were converted into "idealized" concentration curves and graphed versus the experimental scan, as shown for the IDL class on **Fig. 7** and for the LDL class on **Fig. 8.** This type of graphic representation illustrates the comparative agreement between experimental absorbance scans and the theoretically derived boundary curves.

### Subclasses of LDL and IDL and their flotation coefficients

In order to present the correct representation of mean values of naturally occurring flotation coefficients, we took into consideration determinations from the two pilot studies (A and B), shown in **Table 1,** and compared them with corresponding values obtained from the reference (D), shown in **Table 2.**

Table 1, A. The 17 subjects treated with guanadrel were examined before and after 3 months of therapy, so that the calculation of flotation rate means are based on 34 ultracentrifugal analyses.

Table 1, B. The 13 subjects treated with probucol were examined before and after 3 months of therapy, so that the calculations of flotation rate means are based on 26 ultracentrifugal analyses.

Table 1, C. The mean values of flotation rates of LDL and IDL subclasses from groups A and B are very comparable. Therefore, we grouped the patient values and calculated the flotation rates from 60 independent ultracentrifugal analyses of lipoprotein samples of 30 different individuals taken in totally different clinical and metabolic situations and conditions, see Table 1, part C.

Based on approximately 600 analyses primarily from the described clinical metabolic studies on guanadrel (n = 101) and probucol (n = 47) (J. J. Opplt and E. S. Holzberg, unpublished results), diagnostic metabolic

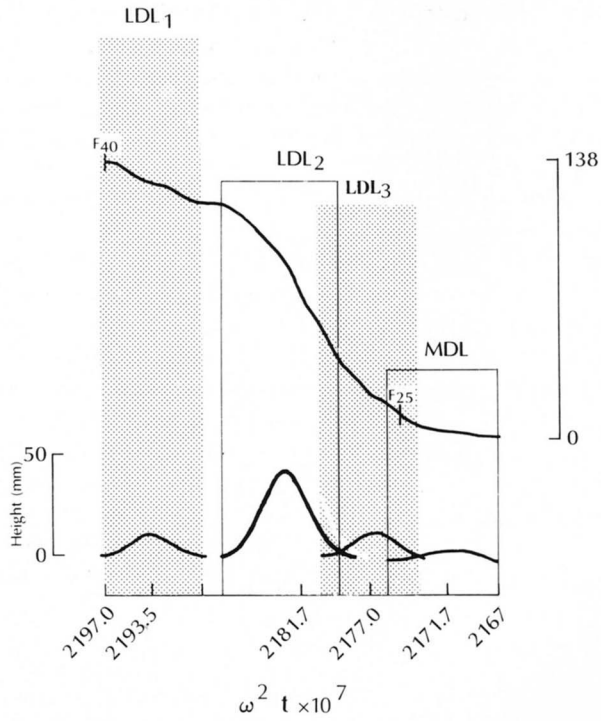


**Fig. 6.** Experimental absorbance scan versus calculated Gaussian concentration gradient curves for LDL subclasses and the MDL class.

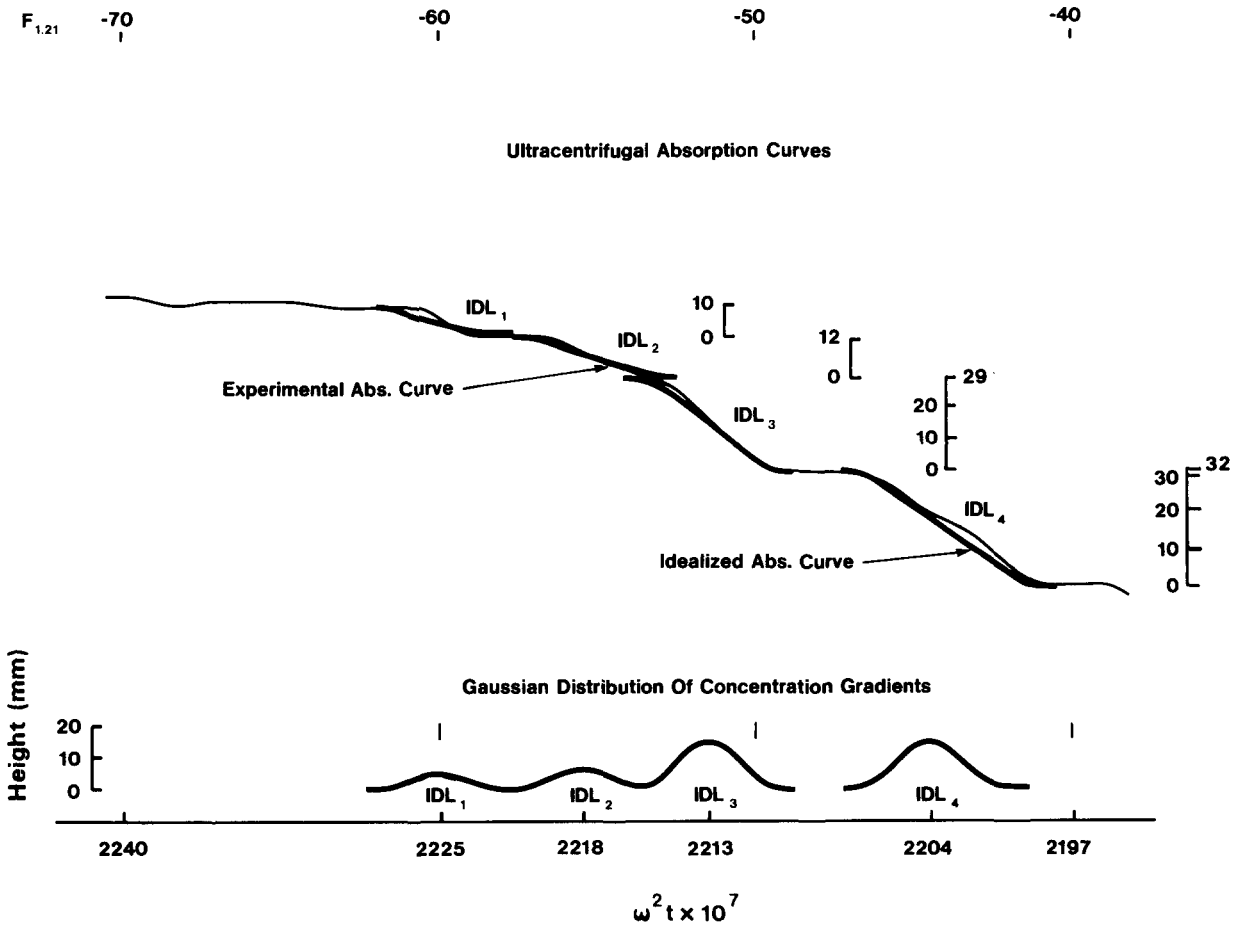


**Fig. 7.** Relationship between experimental absorbance scan of IDL class with derived concentration and concentration gradient boundary curves.

changes in serum lipoproteins are marked only by characteristic changes in concentrations of individual classes, as well as subclasses, while the parameters of their natural flotation rates[4] did not significantly change from their mean values.

Table 2, D. Normolipidemic and normolipoproteinemic individuals were characterized by similar flotation coefficients of their lipoprotein LDL and IDL classes and subclasses. Compared with related parameters, obtained by micro-ultracentrifugal analyses of lipoproteins from patients with or without proven CAD and with dyslipoproteinemia and hyperlipemia of different severity, the differences in analytical values and their statistical deviations are neglible, see Table 2.

This means that not only the severity of a disorder but also the normality of lipoprotein metabolism has no impact on the values of natural flotation coefficients of lipoprotein classes and subclasses.

Reproducibility of the estimation of flotation coefficients of lipoprotein subclasses is approximately comparable to the reproducibility of analyses of flotation coefficients of lipoprotein classes as seen from reproducibility studies (**Table 3**). Judging from the values of achieved standard deviations, the reproducibility of subclasses may be even better than that of classes determined after two to five subsequent ultracentrifugal analyses.

Although the three LDL subclasses were always present in all our studies, we observed the following behavior with the IDL subclasses. *a)* Most consistent was the presence of the $IDL_4$ subclass; *b)* the next most consistent presence was the $IDL_1$ subclass; *c)* the $IDL_3$ subclass appeared to be present most likely in the analyses of significantly dyslipoproteinemic samples, and less likely in normolipoproteinemic samples; and *d)* the presence of the $LDL_2$ subclass was mostly related to the presence of the $LDL_4$ subclass, see Table 3, B.

[4]Using different preparative and analytical ultracentrifugal techniques, we are obliged to distinguish flotation rates instituted arbitrarily (e.g., $S^{o}_{f\,1.063}$) from those flotation rates determined in every case individually (e.g., $F_{1.210}$), according to characteristic inflections on the UV absorbance curve (eventually confirmed by theoretical calculations, as described in this paper).

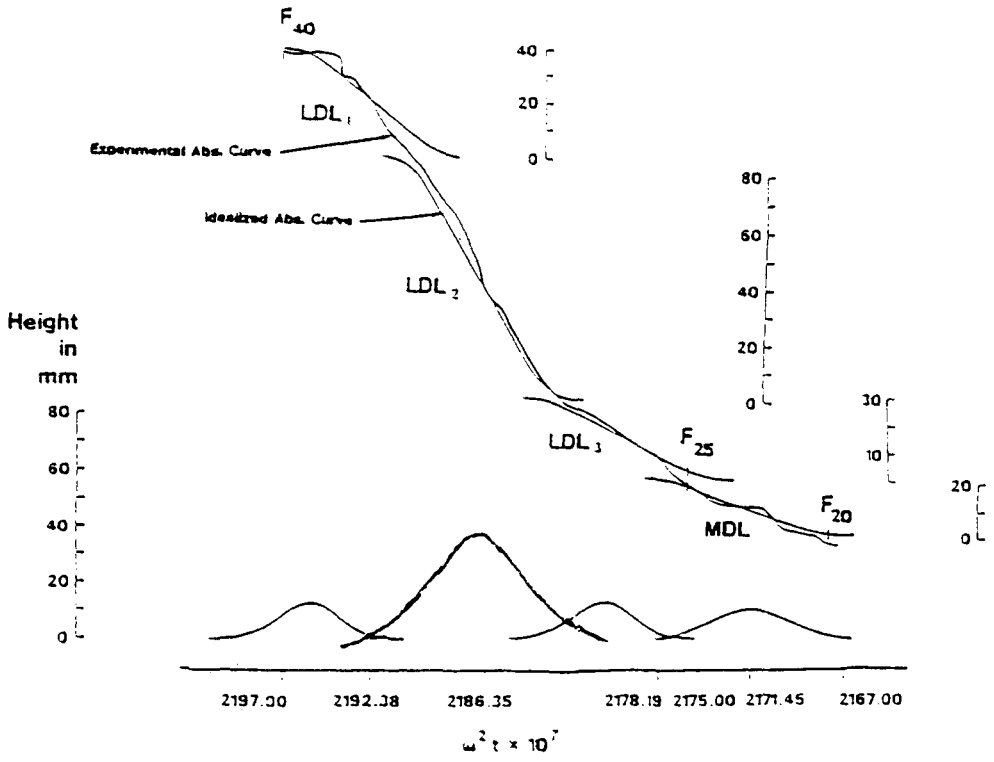


**Fig. 8.** Relationship between experimental absorbance scan of LDL and MDL classes with derived concentration and concentration gradient boundary curves.

Only seldomly could we determine one IDL subclass, e.g. $IDL_1$ (309 FBN), or $IDL_3$ (89 REN). In addition, a finding of two IDL subclasses, e.g. $IDL_1$ and $IDL_3$, was extremely rare (e.g., 92 FFD).

TABLE 1. Subclasses of LDL and IDL and their flotation coefficients

| Class, Subclass | Flotation Coefficient $F_{1.210}$ ± SD | | |
|---|---|---|---|
| | A[a] | B[b] | C[c] |
| IDL | | | |
| $IDL_1$ | 61.6 ± 0.9 | 61.2 ± 1.4 | 61.4 ± 1.1 |
| $IDL_2$ | 53.9 ± 1.0 | 55.3 ± 1.2 | 54.5 ± 1.1 |
| $IDL_3$ | [d] | 50.0 ± 1.0 | 50.0 ± 1.0 |
| $IDL_4$ | 45.6 ± 1.1 | 44.4 ± 1.0 | 45.1 ± 1.1 |
| LDL | | | |
| $LDL_1$ | 37.2 ± 0.6 | 35.9 ± 0.5 | 36.6 ± 0.6 |
| $LDL_2$ | 31.1 ± 0.9 | 29.0 ± 0.9 | 30.2 ± 0.9 |
| $LDL_3$ | 26.9 ± 0.7 | 25.5 ± 0.6 | 26.3 ± 0.7 |

Flotation coefficients were determined as described in Methods. At density 1.21 g/ml, the flotation coefficient range of IDL is 70–40 and the range for LDL is 40–25. Subscript #1 always refers to the subclass with the highest coefficient of flotation.

[a]Mean values of 34 analyses.

[b]Mean values of 26 analyses.

[c]Mean values of combined 60 analyses.

[d]The $IDL_3$ subclass was not analytically detectable in subjects with normal or mildly disordered lipoproteinemia.

The irregular spectrum of IDL lipoprotein subclasses was remarkably stable and reproducible, as we demonstrated, using comparison of analytical values from two to five qualitative and quantitative determinations.

A summary of mean $F_{1.210}$ flotation coefficient values of LDL and IDL subclasses converted to $S^0_{f1.063}$ sedimentation coefficient is shown in **Table 4.** The IDL class, $F_{1.210}$ flotation coefficient range of 63 to 43, corresponded to $S^0_{f1.063}$ flotation coefficient range of 17 to 7, and the LDL class, $F_{1.210}$ flotation coefficient range of 38 to 25, corresponded to $S^0_{f1.063}$ flotation coefficient range of 7 to 1.

## DISCUSSION

The introduced method for mathematical resolution of lipoprotein ultracentrifugal scans is an indirect approach to overcome the current lack of a reliable method for the direct determination of LDL and IDL subclasses. At present, while several methods have been proposed (10–12, 14), they are all of limited use due to their inability to naturally separate the IDL and LDL classes into distinct subclasses.

Subclasses of IDL and LDL are difficult to resolve spontaneously due to their very similar physical and chemical characteristics. For this reason we choose to

TABLE 2. Flotation coefficient in normolipemic individuals

| Class, Subclass | Flotation Coefficient $F_{1.210} \pm SD^a$ D | Flotation Coefficient $S^o_{f\,1.063}{}^b$ |
|---|---|---|
| IDL | | |
| $IDL_1$ | 61.6 ± 1.4 | 16.2 ± 0.6 |
| $IDL_2$ | 54.4 ± 1.5 | 12.6 ± 0.7 |
| $IDL_3$ | [c] | [c] |
| $IDL_4$ | 46.2 ± 1.3 | 8.9 ± 0.6 |
| LDL | | |
| $LDL_1$ | 37.0 ± 0.4 | 5.3 ± 0.1 |
| $LDL_2$ | 31.2 ± 0.9 | 3.2 ± 0.3 |
| $LDL_3$ | 26.6 ± 1.0 | 1.7 ± 0.3 |

Flotation coefficients at density 1.210 g/ml ($F_{1.210}$), determined as described in Methods, were converted to $S^o_{f1.063}$ sedimentation coefficients, using a modification of a published equation ([d], see below (26). Subscript #1 always refers to the subclass with the highest coefficient of flotation.

[a] Mean values of 12 analyses.

[b] $F_{1.21}$ converted into $S^o_{f1.063}$.

[c] The $IDL_3$ subclass was not analytically detectable in subjects with normal or mildly disordered lipoproteinemia.

[d] For converting $F_{1.210}$ flotation coefficients to $S^o_{f1.063}$ sedimentation coefficients,

$$S^o_{f1.063} = F_{1.21} \frac{n_{26°C}}{n_{26°C}} \frac{\varrho_{26°C}}{\varrho_{26°C}} \frac{1 - V_{26°C}}{1 - V_{26°C}}$$

where

$S^o_{f1.063}$ = the flotation coefficient at density 1.063 g/ml and 26°C

$\frac{n_{26°C}}{n_{26°C}}$ = relative viscosity of d 1.21 g/ml medium to that of d 1.063 g/ml medium

$\frac{\varrho_{26°C}}{\varrho_{26°C}}$ = density of 1.21 g/ml medium at 26°C to density of 1.063 g/ml medium at 26°C

$V_{26°C}$ = partial specific volume of lipoproteins in density 1.21 g/ml (and 1.063 g/ml) at 26°C

apply mathematical theory of ultracentrifugation to achieve their separation. The method we have introduced separates ultracentrifugal scans into IDL and LDL subclasses based upon the determined theoretical dimensions of concentration gradient boundary curves of IDL and LDL species. While not exact, this approach enables us to determine IDL and LDL subclasses from experimental ultracentrifugal scans.

While the method is tedious in its initial set-up, once the theoretical boundary dimensions have been calculated and standard plots have been made, our method may be readily applied. Resolution of ultracentrifugation scans into IDL and LDL subclasses can be accomplished within a few minutes.

The approximate coincidence of theoretically derived boundary curves for LDL and IDL subclasses with experimentally obtained ultracentrifugal absorbance scans demonstrates that ultracentrifugal scans of LDL and IDL are a summation of their individual components or subclasses. The coinciding of the two demonstrates the use of the mathematical theory of ultracentrifugation for resolving LDL and IDL boundary regions into their subclass components. Agreement between theoretical and experimental results, however, will always be approximate at best due to inherent variations in experimental conditions.

The basis of the developed method was the application of Eq. 4 (Appendix) for the determination of the theoretical dimensions of IDL and LDL concentration gradient boundaries. During analytical ultracentrifugation, the boundary region (simply referred to as the boundary) represents a transition zone in the cell between the plateau region, a region of equilibrium concentration of actively migrating lipoprotein molecules, and the solvent region. In general, the shape of the boundary in ultracentrifugal scans of sedimentation velocity experiments is controlled by the four factors discussed in detail by Schachman (27). The first is the spreading of the boundary due to lipoprotein class polydispersity. The boundary is a composite of subclass boundary curves. As the faster migrating subclasses (with higher flotation coefficient) tend to move apart from the slower moving subclasses, broadening of the boundary occurs, with flotation coefficient differences producing inflection points in the boundary. The second is spreading of the boundary from diffusive broadening of the composite subclass boundary curves. The third is the dependence of flotation and diffusion coefficients on concentration, and the fourth is the significance of Johnston-Ogston effects on the boundary.

In the formation of LDL and IDL boundaries, heterogeneity and diffusion are the primary factors that control the shape of the observed boundary. Johnston-Ogston effects are not significant, while the effects of concentration on s (= sedimentation coefficient, in Svedberg units) and D (= diffusion coefficient, $cm^2$/sec) can be discounted if these are assumed to be constant (19). In this investigation, we assumed that if we could develop a method by which the effects of diffusion in causing broadening of LDL and IDL boundaries could be substantiate, we would be able to determine the inherent heterogeneity of LDL and IDL and their subclasses.

At present, the effect of the diffusion on broadening of the boundary may only be estimated by inspection and heterogeneity estimated qualitatively. Detection of polydispersity has until recently been carried out by comparing the apparent diffusion coefficient obtained from ultracentrifugal patterns with the measured diffusion coefficient. Schachman (27) stated that if the obtained diffusion coefficient is larger than the measured one, the presence of heterogeneity is indicated.

The methods presented for the analysis of boundaries (16–18) all have major limitations. Computer analysis of the distribution of lipoproteins of density less than

TABLE 3. Reproducibility of flotation coefficients of LDL and IDL subclasses

| Sample | N[a] | Flotation Rate[b] ($F_{1.210}$) LDL$_1$ | LDL$_2$ | LDL$_3$ | |
|---|---|---|---|---|---|
| 52 UKN | 5 | 36.5 ± 0.0 | 30.5 ± 0.5 | 26.1 ± 0.0 | |
| 82 VBN | 2 | 37.2 ± 0.4 | 30.0 ± 0.0 | 26.0 ± 0.0 | |
| 89 REN | 2 | 36.8 ± 0.4 | 30.8 ± 0.4 | 26.0 ± 0.0 | |
| 92 FFD | 3 | 36.3 ± 0.4 | 30.3 ± 0.4 | 26.8 ± 0.4 | |
| 95 EAS | 3 | 36.5 ± 0.0 | 30.5 ± 0.0 | 26.8 ± 0.4 | |
| 309 FBN | 2 | 36.2 ± 0.4 | 29.5 ± 0.0 | 26.0 ± 0.0 | |
| 310 IKT | 3 | 36.5 ± 0.0 | 30.5 ± 0.5 | 25.8 ± 0.3 | |
| | | IDL$_1$ | IDL$_2$ | IDL$_3$ | IDL$_4$ |
| 52 UKN | 5 | 61.1 ± 0.6 | 54.8 ± 0.3 | [c] | 46.0 ± 0.4 |
| 82 VBN | 2 | 61.3 ± 0.4 | 54.5 ± 0.3 | [c] | 44.3 ± 0.4 |
| 89 REN | 2 | [c] | [c] | 50.0 ± 0.7 | [c] |
| 95 EAS | 3 | 61.3 ± 0.4 | [c] | 50.5 ± 0.7 | [c] |
| 309 FBN | 2 | 61.0 ± 0.0 | [c] | [c] | [c] |
| 310 IKT | 3 | 61.0 ± 0.0 | 54.8 ± 0.4 | 49.3 ± 0.4 | 44.0 ± 0.0 |

[a]N, number of scans.
[b]Flotation coefficient was determined as described in Methods.
[c]Subclass not analytically detectable.

1.063 g/ml using schlieren optics was presented by Ewing et al. (16). This procedure consisted of making 29 arbitrary subdivisions of the lipoprotein pattern produced by classic ultracentrifugation technique with schlieren optics. By using standard intervals, and from the height of each subdivision, the approximate area under the integral curve was calculated by rectangular estimation. After correcting for Johnston-Ogston effect and considering F versus concentration effects, their procedure yielded lipoprotein concentrations. This method appears to be limited by the inaccuracy of arbitrary rectangular estimation.

In the method of Oncley (17), lipoprotein distributions according to density and molecular size were mathematically treated as predictable as reference to sedimentation coefficient distributions. The mathematics of this method are complex, with no practical application, thus limiting the possible use of the method.

Anderson et al. (18) introduced a method for the analysis of the major components of HDL from boundary schlieren patterns. By using reference schlieren patterns of HDL subclasses, the original HDL pattern was reconstructed. The reference schlieren patterns were obtained separately by averaging the patterns of derived HDL subclasses, using the method of Ewing et al. (16). Therefore, one of the major limitations of this method is applicability to LDL and IDL boundary curves.

Swinkels et al. (14) presented a computerized mathematical modeling procedure for deconvolution analysis of schlieren boundary curves of LDL into Gaussian components. A major inaccuracy of this procedure lies in its lack of any physical basis for deriving the Gaussian curves. At best, this method offers only an approximation of the correct curves.

The above described methods are only qualitative at best, without the possibility of natural determination of the shape of boundaries from diffusive spreading. However, the results of Swinkels' procedure compare favorably with results of the present study.

The design of this project also included the demonstration of the applicability of mathematical theory of ultracentrifugation for predicting of significant broadening of Gaussian curves of LDL and IDL subclasses due to diffusion. Fundamental to the application of mathematical theory of ultracentrifugation is the general differential equation of Lamm (28) describing the sedimentation of a single homogeneous solute in the sector-shaped cell under ultracentrifugal forces. Lamm's differential equation

TABLE 4. Mean flotation coefficients of LDL and IDL subclasses presented at two standard densities

| Class, Subclass | Flotation Coefficient $F_{1.210}$ ± SD | $S^o_{f1.063}$ ± SD |
|---|---|---|
| IDL | | |
| IDL$_1$ | 61.4 ± 1.1 | 16.1 ± 0.5 |
| IDL$_2$ | 54.5 ± 1.1 | 12.7 ± 0.5 |
| IDL$_3$ | 50.0 ± 1.0 | 10.6 ± 0.4 |
| IDL$_4$ | 45.1 ± 1.1 | 8.4 ± 0.5 |
| LDL | | |
| LDL$_1$ | 36.6 ± 0.6 | 5.1 ± 0.2 |
| LDL$_2$ | 30.2 ± 0.9 | 2.8 ± 0.3 |
| LDL$_3$ | 26.3 ± 0.7 | 1.6 ± 0.2 |

Flotation coefficients at density 1.210 g/ml ($F_{1.210}$), determined as described in Methods, were converted to $S^o_{f1.063}$ sedimentation coefficients using the equation presented in Table 2. Values are means of combined 60 analyses.

brought the effects of sedimentation, diffusion, angular velocity, and equations of flux together into an equation relating concentration changes of solute with time.

Other investigators have applied solutions of Lamm's differential equation for analyzing sedimentation velocity data for macromolecular systems. Faxen (25) derived an approximate solution of Lamm's equation, under the constraints that both the flotation rate and the diffusion coefficient are independent of concentration. This solution was able to explain that concentration gradient boundary curves calculated for sedimenting proteins were Gaussian in form, with only very slight corrections. However, due to the assumptions used by Faxen (25), his solution is limited only to the early stages of velocity ultracentrifugation of solutes characterized by sufficiently large molecular size of their particles.

Fujita (19) and Williams et al. (20) later extended Faxen's solution by deriving an exact solution of Lamm's equation. Similarly, Fujita (19) deduced that the concentration gradient boundary curve predicted from his solution will be Gaussian in form.

We conclude that, by modifying the equation of Fujita (19) for flotating lipoproteins, we derive an equation useful for the calculation of theoretical concentration gradient boundary curves that appear to be similar to Gaussian curves in form. By using the modified equation (and following the procedure outlined in Methods), we were able to analyze the boundary regions of LDL and IDL from experimental ultracentrifugal absorbance scans, and then determine the LDL and IDL subclasses as true Gaussian boundary curves.

Analysis of ultracentrifugal absorbance scans of LDL and IDL revealed the boundary region of LDL to be the summation of three subclasses of LDL, and the boundary region of IDL to be most frequently the summation of two to four subclasses of IDL. Most of the observed IDL and LDL subclass ultracentrifugal flotation coefficient ranges are comparable to those published by other authors during the last two decades.

The LDL class of plasma lipoproteins floats in the density range 1.019–1.063 g/ml. This physical continuum of LDL forms a spectrum of particles varying in size, hydrated density, and chemical composition.

LDL in the 1.019–1.063 g/ml density range are usually referred to as low density classes = $LDL_{2,3}$. The 1.006–1.019 g/ml density range (IDL) was in the past called low density lipoprotein = $LDL_1$.

IDL and LDL were referred to by Gofman et al. (29) as the ultracentrifugally separated lipoproteins with $S^0_{f1.063}$ rates of 20–12 and 12–0, respectively. Krauss and Burke (12) have reported LDL to comprise the 10–0 $S^0_{f1.063}$ range. Our results indicate that IDL and LDL classes are better described by $S^0_{f1.063}$ ranges for IDL of 17–7 and for LDL of 7–1. The differences between our ranges and those of Gofman et al. (29) and Krauss and Burke (12) may be attributable to our reference of $IDL_4$ as IDL subclass of $S^0_{f1.063}$ 10–7 versus reference as the $LDL_1$ subclass.

The subclasses of LDL were described first in 1970 by Adams and Schumaker (30). Until that time, the LDL class had been thought to be a continuous distribution of material with respect to composition and density. Adams and Schumaker (30) found that discrete components (usually two were observed, using the banding techniques) do exist in the LDL class, which are heterogeneous with respect to density.

Lindgren, Jensen, and Hatch (31) showed in 1972 that an inverse relationship exists between molecular weight and density for these components (see **Table 5**) and that there are usually three components. Fisher (7), Hammond and Fisher (32), and Hammond et al. (33) fractionated the 1.006–1.09 g/ml density range (e.g., IDL and LDL) into three subfractions by preparative flotation. The flotation characteristics in each subfraction were then analyzed by analytical ultracentrifugation. Two subspecies of lipoproteins were apparent in the 1.006–1.019 g/ml density range and three in the 1.019–1.063 g/ml density range. In 1971, Hammond and Fisher (32) determined their molecular weights: 4.9, 4.3, 3.2, 2.5, and 1.3 million daltons (multiples of $6.25 \times 10^5$ g per mole of lipoprotein). The polydispersity of LDL was further related to increased plasma concentrations of VLDL (mostly found in patients with hyperlipoproteinemia type IIB and IV, in 78% of subjects with hypertriglyceridemia) (33). Fisher (7) postulated that these polydisperse subspecies of the LDL class were related to each other as precursor to product, with the larger lipoproteins being converted to the smaller lipoproteins of the class.

The above findings were confirmed by Nelson and Morris (5) who separated LDL into a fast component of $S^0_{f1.2KBR}$ 40 (= $F^0_{1.210}$) and a slow component of $S^0_{f1.2KBR}$ 45.5 (= $F^0_{1.210}$) which was correlated with serum triglyceride values.

TABLE 5. Comparison of density, flotation coefficient, and molecular weight of Lindgren's LDL fractions (31)

| Component | $S^0_{f1.063}$[a] Rate | $S^0_{f1.063}$[a] Peak | $F_{1.21}$[b] Peak | $\varrho$[c] | M.W.[d] |
|---|---|---|---|---|---|
| Fraction I[e] | 10–20 | 13.5 | 56.2 | 1.009 | 3.2 |
| Fraction II | 6–12 | 6.9 | 42.3 | 1.027 | 2.2 |
| Fraction III | 3.5–6.5 | 4.5 | 34.7 | 1.037 | 1.9 |

[a]Flotation rate at density 1.063 g/ml.
[b]Flotation rate at density 1.210 g/ml.
[c]Hydrated density (g/ml mean values).
[d]Molecular weight (in millions).
[e]Fraction I presently belongs to the IDL density range.

TABLE 6. Flotation coefficient of LDL and IDL subclasses isolated by Lee and Downs (11)

| Class | Ultracentr. Layer | Subclass | A[a] | | B[b] | | C[c] | |
|---|---|---|---|---|---|---|---|---|
| | | | $S^o_{f1.063}$ | $F_{1.210}$ | $S^o_{f1.063}$ | $F_{1.210}$ | $S^o_{f1.063}$ | $F_{1.210}$ |
| IDL | 1 | VLDL | 14.3 | 48.8 | 20.0 | 68.0 | 16.0 | 53.8 |
| IDL | 2 | $LDL_1$ | 11.4 | 41.6 | 12.3 | 41.6 | 12.3 | 43.7 |
| LDL | 2 | | 8.3 | 34.6 | 8.2 | 34.4 | | |
| LDL | 3 | | 6.0 | 30.1 | 6.7 | 31.5 | 6.3 | 30.7 |
| LDL | 4 | | 5.3 | 28.7 | 4.5 | 27.2 | 4.5 | 27.2 |

[a]Analysis of one healthy man.
[b]Analysis of one patient with type III hyperlipemia.
[c]Analysis of one patient with type IV hyperlipemia.

Lee and Alaupovic (2) used sequential preparative flotation to arbitrarily fractionate the 1.006–1.019 g/ml density range into two subfractions and the 1.019–1.063 g/ml range into five subfractions.

Using the knowledge that heterogeneity exists in LDL, Rubenstein (34) applied ion-exchange chromatography to subdivide the entire complex into the so called $LDL_1$ unit and three chromatographic subunits of the $LDL_{2,3}$ complex, e.g., into 1 + 3 fractions.

Using density gradient ultracentrifugation, Adams and Schumaker (30), as well as Shen et al. (6), Krauss and Burke (12), and Lee and Downs (11), all demonstrated the presence of isopycnic bands in the LDL class.

For example, Lee and Downs (11) isolated four individual bands by preparative ultracentrifugation, and, after analysis using analytical ultracentrifugation, they characterized one band as consisting of a mixture of VLDL and LDL, and the other three bands as $LDL_{1-3}$ subspecies, with the presence of two additional subspecies in one of these bands (**Table 6**).

On the other hand, Krauss and Burke (12) observed multiple bands in the LDL class (**Table 7**). Finally, they also reported four LDL electrophoretic subfractions (LDL I–LDL IV) using nondenaturing electrophoresis of serum lipoproteins on 2–16% polyacrylamide gradient gels (12).

The LDL subclass may also possess different physicochemical properties (e.g., chemical composition, particle size, molecular weight, and conformation) under different pathological conditions.

Hammond and Fisher (32) reclassified the LDL class as a family of monodisperse LDL subclasses of molecular weight 2.1–3.9 × $10^6$ and polydisperse LDL subclasses (in about 80% of individuals with hyperglyceridemia and increased VLDL concentration). Fisher (7) later suggested that there is an increased association of polydisperse LDL with atherosclerosis in hypertriglyceridemic diabetics.

In the 1980s, the research of subclasses of atherogenic lipoprotein classes developed further, using mostly combinations of ultracentrifugal and electrophoretic techniques (mainly agarose and polyacrylamide gels). New characteristics of lipoprotein subclasses, this time using mainly electrophoretic techniques, completed the ultracentrifugal parameters determined during the previous decade.

The above studies have served to document close correlations of our results with corresponding values presented by earlier workers (7, 30–36) in research of structural heterogeneity of the spectrum of particles that constitute the LDL and IDL classes of serum lipoproteins.

TABLE 7. Flotation coefficient of four LDL subclasses isolated by Krauss and Burke (12)

| Class, Subclass | Flotation Coefficient | |
|---|---|---|
| | $S^o_{f1.063}$[a] | $F_{1.210}$[b] |
| LDL | | |
| $LDL_1$ | 10–7.5 | 38.5–33.1 |
| $LDL_2$ | 7.5–5.7 | 33.1–29.5 |
| $LDL_3$ | 5.7–4.2 | 29.5–26.6 |
| $LDL_4$ | 4.0–0.0 | 26.2–19.0 |

[a]Values from 12 analyses.
[b]$S^o_{f1.063}$ converted into $F_{1.210}$.

## APPENDIX

**Derivation of reference theoretical IDL and LDL boundary curves**

Fujita's equation (19, 20) for predicting boundary patterns of sedimenting proteins may be written in the form:

$$\frac{\delta(c/c_o)}{\delta(r/r_o)} = [e^{-1.5\tau}/(\pi\epsilon(1 - e^{-\tau}))^{1/2}]e^{-\xi^2} \qquad Eq.\ 1)$$

where:

$\xi = [1 - e^{-\tau}/2(r/r_o)][\epsilon(1 - e^{-\tau})]^{-1/2}$
$\epsilon = 2D/\omega^2 r^2_o s$ (dimensionless parameter)
$\tau = 2\omega^2 ts$ (dimensionless parameter)
r = radial distance to the boundary (cm)
$r_o$ = radial distance to the meniscus (cm)
s = sedimentation coefficient in Svedberg units
D = diffusion coefficient ($cm^2$/sec)
$\omega$ = angular velocity (radians/sec)
t = centrifugal time in seconds for attainment of boundary position
c = lipoprotein concentration at time t
$c_o$ = initial lipoprotein concentration
$\pi$ = 3.14

Equation 1 was found to be applicable to flotating lipoproteins by substituting $r_B$ for $r_o$, where:

$r_B$ = radial position of cell bottom
$-s$ = ultracentrifugal flotation rate in negative Svedberg units
D = diffusion coefficient values used were derived from published values (32, 33)

To express lipoprotein flotation in flotation coefficient units, versus Svedberg units, it was necessary to change Eq. 1 to Eq. 2 by:

1) converting flotation coefficient values in negative Svedberg units ($-s$) to F units,
2) replacing $[e^{-1.5\tau}/(\pi\epsilon(1 - e^{-\tau}))^{1/2}]$ by $[e^{1.5\tau}/(-\pi\epsilon(1 - e^{\tau}))^{1/2}]$ in Eq. 2, and
3) by converting $\xi = [1 - e^{-\tau/2}(r/r_o)][\epsilon(1 - e^{-\tau})]^{-1/2}$ in Eq. 1 to $\xi = [1 - e^{\tau/2}(r_x/r_B)][-\epsilon(1 - e^{\tau})]^{-1/2}$ in Eq. 2.

where:

$r_x$ = radial position in the cell for lipoprotein boundary with flotation coefficient F at time t
$\epsilon = 2D/\omega^2 r_B^2 F$
$\tau = 2\omega^2 tF$

The two latter modifications account for the reverse movement of particles undergoing flotation in relation to sedimentation.

These modifications of Eq. 1 yield Eq. 2,

$$\frac{\delta(c/c_B)}{\delta(r/r_B)} = [e^{1.5\tau}/(-\pi\epsilon(1 - e^{\tau}))^{1/2}]e^{-\xi^2} \qquad \textit{Eq. 2)}$$

### Construction of theoretical IDL and LDL boundary curves

Reference concentration gradient boundary curves for IDL and LDL lipoproteins are derived using Eq. 2. as the concentration gradient (dc/dr) versus radial distance. An example of the calculation of one value of dc/dr for a specified radial position is shown in **Table 8.**

TABLE 8. Calculation of concentration gradient

A: Ultracentrifugation parameters and lipoprotein property values for calculation

$F_{1.21} = 40 \cdot 10^{-13}$ sec (flotation coefficient of boundary)
$r_x = 6.593$ cm (an example boundary position)
$r_B = 7.20$ cm (radial position of cell bottom)
$\omega^2 = (52{,}640 \text{ rpm})^2 = 3.03 \cdot 10^7$ (radians/sec)$^2$
$\omega^2 t = 2197 \cdot 10^7$ rad$^2$/sec
$D = 2.11 \cdot 10^{-7}$ cm$^2$/sec
$\tau = 2 \cdot (\omega^2 t) \cdot F_{1.21} = 0.176$
$\epsilon = \dfrac{2\ D}{F_{1.21} \cdot \omega^2 \cdot (r_B)^2} = 6.72 \cdot 10^{-5}$

B: Example of calculation of concentration gradient at a specified radial position

Eq. 2 = $\delta c/\delta r = [\epsilon^{1.5\tau}/(-\pi\epsilon(1 - e^{\tau}))^{1/2}\ e^{-\xi^2}$
$\delta c/\delta r = [e^{(0.264)}]/[-(3.14)(6.72 \cdot 10^{-5})(-0.192)]^{1/2}\ e^{-\xi^2}$
$\delta c/\delta r = [204.1] \cdot e^{-[1 - e^{\tau/2}(r_x/r_B)][-\epsilon(1 - e^{\tau})]^{1/2}]^2}$

| $\delta c/\delta r$ = | Maximum Gradient Height | Percentage of Gradient at $r_x$ = | Concentration Gradient at $r_x$ |
|---|---|---|---|
| $\delta c/\delta r$ = | 204.1 | 1.0 = | 204.1 |

The calculated boundary curves are graphed as dc/dr versus the radial distance $\pm (r_\star - r_x)$, with $r_\star$ representing the apex of IDL and LDL boundaries. At the apex of IDL and LDL boundaries, $r_\star = r_x$ and $r_\star - r_x = 0$.

The apex of IDL and LDL boundaries was calculated using Eq. 3,

$$r_\star = r_B \cdot \exp^{-[F \cdot \omega^2 \cdot t \cdot 10^{-13}]} \qquad \textit{Eq. 3)}$$

### Theoretical concentration distribution of IDL and LDL boundaries

The theoretical concentration distribution of IDL and LDL boundaries is calculated using Eq. 4, an extension of Eq. 2,

$$\%\text{ of Max. Gradient at } r_\star - r_x \text{ distances} = \exp^{-\frac{[1 - (e^{2\omega^2 tF/2}) \cdot (r_x/r_B)]^2}{[(-2D/F \cdot \omega^2 \cdot r^2) \cdot (1 - e^{2\omega tF})^2]^{1/2}}} \qquad \textit{Eq. 4)}$$

In Eq. 2. there appear two distinct factors. The exponential term $\exp^{-\xi^2}$, calculates the fractional percentage of the concentration gradient about its apex. The remaining factor, $e^{1.5\tau}/(-\pi\epsilon(1 - e^{\tau}))^{1/2}$, calculates the maximum height of the gradient. Factor two was normalized to a constant value of one, to obtain Eq. 4. Eq. 4 is used to calculate the theoretical boundary gradient distribution of lipoprotein species.

### Determination of theoretical IDL and LDL boundary widths

The width of IDL and LDL boundaries is taken as the radial distance within which lies 95% of the concentration gradient. This distance corresponds with 2 times the radial distance from the boundary apex to the position at which 2.5% of the lipoprotein species exists ($r_{2.5\%}$). Using Eq. 4, boundary percentages at various radial distances from the apex are calculated until the $r_{2.5\%}$ radial distance is determined. An example of verification of $r_{2.5\%}$ is shown in **Table 9, b.** An example of the calcu-

TABLE 9. Determination of boundary width

A: Ultracentrifugation parameters and lipoprotein property values

$r_\bullet$ = 6.593 cm (radial position of boundary's apex)
$r_x$ = 6.637 cm (previously determined $r_{2.5\%}$ position at which 2.5% of boundary is present)

(All other parameters are as given in Table 8)

B: Verification of $r_{2.5\%}$ radial position

Eq. 4 = $e^{-[(1 - e^{\tau/2}(r_x/r_B))][-\epsilon(1 - e^{\tau})]^{1/2}]^2}$
$= e^{-[1 - ((1.092)(6.637/7.2))(-\epsilon(1 - e^{-\tau}))^{1/2}]^2}$
$= e^{-[(1 - 1.00692)/((-6.72\ 10^{-5})(-0.192)^{1/2}]^2}$
$= e^{-[-6.92 \cdot 10^{-3}/3.59 \cdot 10^{-3}]^2}$
$= e^{-[-1.93]^2} = 3^{-3.7} = 0.024$

C: Calculation of boundary width

Boundary width = $2 \times (r_\star - r_x)$ =
$= 2 \times (6.593 \text{ cm} - 6.637 \text{ cm}) = 2 \times 0.044$ cm
$= 0.088$ cm $\times$ (1 $\omega^2 t/0.011$ cm)
$= 8.0\ \omega^2 t$ (parameter applied to experimental scan)

D: Boundary range

Boundary range = $\pm (r_\star$ − boundary width/2)
$= (r_\star - 0.044 \text{ cm}) \rightarrow (r_\star + 0.044 \text{ cm})$
$= (r_\star - 4.0\ \omega^2 t) \rightarrow (r_\star + 4.0\ \omega^2 t)$

lation of the width of a boundary in both $\omega^2 t$ and cm values is shown in Table 9, c.

**Determination of experimental IDL and LDL subclasses**

Gaussian boundary curves of IDL and LDL subclasses were resolved from recorded $\omega^2 t = 2098 \cdot 10^7$ rad²/sec cell scans of absorbance versus $\omega^2 t$ (radial distance in the cell) by using the following six steps.

First, the apexes of LDL and IDL boundary curves were determined by enlarging experimental linear absorbance scans ten times. The boundary's apex was taken as the position on the x-axis of the scan, one-half the distance between two inflection points (Fig. 1a).

The apex may also be estimated from the first derivative plot of the linear scan. Both the height of the scan (in mm) and the corresponding $\omega^2 t$ value are put into a computer program for a number of points on the enlarged scan. The program yields a plot of the first derivative, with observed maxima taken as the apex of a boundary.

Second, the determined apex position of each boundary was marked on the experimental absorbance scans and the corresponding $F_{1.21}$ flotation coefficient was calculated using Eq. 5.

$$F_{1.21} = \frac{\ln (r_\star / r_B)}{(\omega^2 t) \cdot 10^{-13}} \qquad Eq.\ 5)$$

Third, the distribution of each boundary about its apex is determined using Eq. 4 to calculate the percentage of the concentration gradient at $\pm (r_\star - r_x)$ distances from the boundary apex (Fig. 1b). Calculation of the boundary concentration percentage at which $r_\star - r_x = r_{2.5\%}$ is shown in Table 9, c.

An alternative to this procedure is to use the standard relationships of concentration gradient distribution versus radial distance from the apex that are derived from Eq. 4. Using these relationships, the percentage distribution of the boundary about its apex is readily obtained by drawing a vertical line (corresponding to the flotation coefficient of a boundary) through the linear plots. The intersection of the vertical line with the linear relationships corresponds to the concentration gradient boundary percentage at the specific distance from the boundary apex.

Fourth, from step 3, the $r_{2.5\%}$ distance from the boundary apex to the radial position at which 2.5% of the lipoprotein species exists was determined. These positions, representing the upper and lower ends of a boundary, were marked on the experimental scan (Fig. 1c). The distance between the boundary positions, two times the $r_{2.5\%}$ distance, represents the boundary scan and was taken as the width of the boundary.

Fifth, the height of the boundary concentration gradient curve was taken as one-half the vertical distance from the left end of that scan to the right end on the experimental scan (Fig. 1c).

Sixth, the dimension of each boundary was obtained by multiplying the determined boundary distribution in step 3 times the determined midpoint height of the gradient curve. This yields the form (height in mm) of the concentration gradient boundary curve at $\pm (r_\star - r_x)$ distances from the apex of the boundary (Fig. 1d).

The authors wish thank Professor Verne Schumaker, Professor of Chemistry and Biochemistry, University of California, Professor Jiri Hajek, Professor of Mathematics, Case Western Reserve University, Dr. Glen Richards, VA Medical Center, Dallas, Texas, and the late Professor Emeritus Lena A. Lewis, Cleveland State University, for reading the manuscript and assistance with its preparation.

*Manuscript received 15 September 1992, in revised form 13 April 1993, and in re-revised form 7 October 1993.*

## REFERENCES

1. Lindgren, F. T., L. C. Jensen, R. D. Willis, and N. K. Freeman. 1969. Flotation rates, molecular weights, and hydrated densities of the low density lipoproteins. *Lipids.* **4:** 337–344.
2. Lee, D. M., and P. Alaupovic. 1970. Studies of the composition and structure of plasma lipoproteins. Isolation, composition and immunochemical characterization of low density lipoprotein subfractions of human plasma. *Biochemistry.* **9:** 2244–2252.
3. Fisher, W. R., M. G. Hammond, and G. L. Warmke. 1972. Measurements of molecular weight variability of plasma low density lipoproteins among normals and subjects with hyper-$\beta$-lipoproteinemia. *Biochemistry.* **11:** 519–525.
4. Lee, D. M. 1976. Isolation and characterization of low density lipoproteins. *In* Low Density Lipoproteins. C. E. Day and R. S. Levy, editors. Plenum Press, New York, NY. 3–47.
5. Nelson, C. A., and M. D. Morris. 1977. The ultracentrifugal heterogeneity of serum low density lipoproteins in normal humans. *Biochim. Med.* **18:** 1–9.
6. Shen, M. M. S., R. M. Krauss, F. T. Lindgren, and T. M. Forte. 1981. Heterogeneity of serum low density lipoproteins in normal human subjects. *J. Lipid Res.* **22:** 236–244.
7. Fisher, W. R. 1983. Heterogeneity of plasma low density lipoproteins manifestations of the physiologic phenomenon in man. *Metabolism.* **32:** 283–291.
8. Teng, B., G. R. Thompson, A. D. Sniderman, T. M. Forte, R. M. Krauss, and P. O. Kwiterovich. 1983. Composition and distribution of low density lipoprotein fractions in hyperapobetalipoproteinemia, normolipidemia and familial hypercholesterolemia. *Proc. Natl. Acad. Sci. USA.* **80:** 6662–6666.
9. Chapman, M. J., P. M. Laplaud, G. Luc, P. Forgez, E. Bruckert, S. Goulinet, and D. Lagrange. 1988. Further resolution of the low density lipoprotein spectrum in normal human plasma: physicochemical characteristics of discrete subspecies separated by density gradient ultracentrifugation. *J. Lipid Res.* **29:** 442–458.
10. McNamara, J. R., H. Campos, J. M. Ordovas, J. Peterson, P. W. F. Wilson, and E. J. Schaefer. 1987. Effect of gender, age, and lipid status on low density lipoprotein sub-fraction distribution. *Arteriosclerosis* **7:** 483–490.
11. Lee, D. M., and D. Downs. 1982. A quick and large-scale density gradient subfractionation method for low density lipoproteins. *J. Lipid Res.* **23:** 14–27.
12. Krauss, R. M., and D. J. Burke. 1982. Identification of multiple subclasses of plasma low density in normal humans. *J. Lipid Res.* **23:** 97–104.
13. Swinkels, D. W., H. L. M. Hak-Lemmers, and P. N. M. Demacker. 1987. Single spin density gradient ultracentrifugation method for the detection and isolation of light and heavy low density lipoprotein subfractions. *J. Lipid Res.* **28:** 1233–1239.
14. Swinkels, D. W., P. N. M. Demacker, J. C. M. Hendricks, and A. van't Laar. 1989. Low density lipoprotein subfractions and relationship to other risk factors for coronary artery disease in healthy individuals. *Arteriosclerosis.* **9:** 604–613.
15. Musliner, T. A., C. Giotas, and R. M. Krauss. 1986. Presence of multiple subpopulations of lipoproteins of intermediate density in normal subjects. *Arteriosclerosis.* **6:** 79–87.
16. Ewing, A. M., N. K. Freeman, and F. T. Lindgren. 1965. The analysis of human serum lipoprotein distribution. *Adv. Lipid Res.* **3:** 25–62.
17. Oncley, J. L. 1969. Evaluation of lipoprotein size-density distribution from sedimentation coefficient distributions obtained at several solvent densities. I. Theory. *Biopolymers.* **7:** 119–132.
18. Anderson, D. W., A. V. Nichols, S. S. Pan, and F. T. Lind-

gren. 1978. High density lipoprotein distribution resolution in determination of three major components in a normal population sample. *Atherosclerosis.* **29:** 161–179.
19. Fujita, H. 1956. Effects of a concentration dependence of the sedimentation coefficient in velocity ultracentrifugation. *J. Chem. Phys.* **24:** 1084–1090.
20. Williams, J. W., E. V. Van Holde, R. L. Baldwin, and H. Fujita. 1958. The theory of sedimentation analysis. *Chem. Rev.* **58:** 715–806.
21. LeLorier, J., S. DuBreuil-Quidoz, S. Lussier-Cacan, Y. S. Huang, and J. Davignon. 1977. Diet and probucol in lowering cholesterol concentrations. Additive effects on plasma cholesterol concentrations in patients with familial type II hyperlipoproteinemia. *Arch. Intern. Med.* **137:** 1429–1434.
22. Lewis, L. A., A. A. Green, and I. H. Page. 1952. Ultracentrifugal lipoprotein patterns of serum of normal, hypertensive and hypothyroid animals. *Am. J. Physiol.* **171:** 391–400.
23. Opplt, J. J., and R. C. Bahler. 1982. Ultracentrifugal study of metabolic effects of probucol: plasma lipoproteins in patients with proven coronary artery disease. *Artery.* **10:** 108–130.
24. Young, R. 1978. Micro-ultracentrifugal analysis of lipoproteins and its application to a clinical study. Ph.D. Thesis. Cleveland State University, Cleveland, Ohio.
25. Faxen, H. 1929. Uber eine Differentialgleichung aus der Physikalischen Chemie. *Arkiv. Mat. Astron. Fysik.* **21B:** No. 3.
26. Svedberg, T., and K. O. Pedersen. 1940. The Ultracentrifuge. Oxford University Press, New York. p. 36.
27. Schachman, H. K. 1959. Ultracentrifugation in Biochemistry. Academic Press, New York.
28. Lamm, O. 1929. Die Differentialgleichung der Ultrazentrifugierung. *Arkiv. Mat. Astron. Fysik.* **21B:** No. 2.
29. Gofman, J. W., H. B. Jones, F. T. Lindgren, T. P. Lyon, and H. A. Elliot. 1950. Blood lipids and human atherosclerosis. *Circulation.* **2:** 161–178.
30. Adams, G. H., and V. N. Schumaker. 1970. Equilibrium banding of low-density lipoproteins. III. Studies on normal individuals and the effects of diet and heparin-induced lipase. *Biochim. Biophys. Acta.* **210:** 462–272.
31. Lindgren, F. T., L. C. Jensen, and F. T. Hatch. 1972. Monograph: Blood Lipids and Lipoproteins. Chapter 5. The isolation and quantitative analysis of serum lipoproteins. G. J. Nelson, editor. John Wiley & Sons, Inc. Publishers, New York.
32. Hammond, M. G., and W. R. Fisher. 1971. The characterization of a discrete series of low density lipoproteins in the disease hyper-pre-beta-lipoproteinemia. *J. Biol. Chem.* **246:** 5454–5465.
33. Hammond, M. G., M. C. Mengel, G. L. Warmke, and W. R. Fisher. 1977. Macromolecular dispersion of human plasma low-density lipoproteins in hyperlipoproteinemia. *Metabolism.* **26:** 1231–1242.
34. Rubenstein, B. 1978. Heterogeneity of human plasma low density lipoprotein. *Can. J. Biochem.* **56:** 977–980.
35. Fisher, W. R., M. E. Grande, and J. L. Mauldin. 1971. Hydrodynamic studies of human low density lipoproteins. *Biochemistry.* **10:** 1622–1628.
36. Lee, D. M., and P. Alaupovic. 1974. Physicochemical properties of low-density lipoproteins of normal human plasma. *Biochem. J.* **137:** 155–167.